PHYSICAL REVIEW E **70**, 065601(R) (2004)

Negative index lens aberrations

D. Schurig* and D. R. Smith*
Physics Department, University of California, San Diego, La Jolla, California, 92093, USA
(Received 1 April 2004; published 17 December 2004)

We examine the Seidel aberrations of thin spherical lenses composed of media with refractive index not restricted to be positive. We find that consideration of this expanded parameter space allows for the reduction or elimination of more aberrations than is possible with only positive index media. In particular, we find that spherical lenses possessing real aplanatic focal points are possible only with a negative index. We perform ray tracing, using a custom code that relies only on Maxwell's equations and conservation of energy, that confirms the results of the aberration calculations.

DOI: 10.1103/PhysRevE.70.065601 PACS number(s): 42.15.Fr, 42.70.Qs, 42.79.Bh

In 1968, Veselago proposed the idea that a material could have a negative index of refraction, and described how this would impact many basic electromagnetic phenomena [1]. In recent years, there has been great interest in this subject due to experimental demonstrations of negative index artificial materials [2], and the introduction of the perfect lens concept [3]. A perfect lens is a *flat* slab of index minus one, which can focus radiation from nearby objects with the resolution exceeding the diffraction limit.

However, the perfect lens, which can be correctly described as antivacuum [4], has little in common with traditional optical elements. While it does offer a working distance equal to its thickness, it does not possess a focal length. Radiation from distant sources is not focused by a perfect lens; plane waves remain plane waves after traversal. Many applications (cameras, telescopes, antennas, etc.) require the ability to focus radiation from distant objects. As with traditional positive index lenses, this can be achieved with negative index media by using curved surfaces [5]. While it is impossible to achieve subdiffraction image resolution of distant sources, spherical profile lenses composed of negative index media have several advantages over their positive index counterparts: they are more compact, they can be perfectly matched to free space, and here we demonstrate that they can also have superior focusing performance.

The monochromatic imaging quality of a lens can be characterized by the five Seidel aberrations: spherical, coma, astigmatism, field curvature, and distortion. These well-known corrections to the simple Gaussian optical formulas are calculated from a fourth-order expansion of the deviation of a wave front from spherical. (A spherical wave front converges to an ideal point focus in ray optics.) The coefficients in this expansion quantify the nonideal focusing properties of an optical element for a given object and image position [6]. We find that there is an asymmetry of several of the Seidel aberrations with respect to index about zero. Considering that an interface with a relative index of +1 is inert and one of relative index −1 is strongly refractive, this asymmetry is not surprising. However, our conclusion that the asymmetry can yield superior focusing properties for negative index lenses is not obvious.

*Present address: Department of Electrical and Computer Engineering, Duke University, Box 90291, Durham, NC 27708, USA.

We note that negative index media are necessarily frequency dispersive, which implies increased chromatic aberration and reduced bandwidth. However, diffractive optics, which possess a similar limitation, have found utility in narrow band applications [7].

To confirm the analytical aberration results, we developed a custom ray tracing code that does not rely on the sign of the index to determine the path of the ray, but relies only on the permittivity, ε, the permeability, μ, Maxwell's equations, and conservation of energy.

Between interfaces, in homogenous media, the ray propagates in a straight line following the direction of the Poynting vector. Refraction across an interface, from a region labeled 1 into a region labeled 2, is handled as follows. Wave solutions are sought that satisfy the dispersion relation (obtained from Maxwell's equations) in region 2,

$$(c^2/\omega^2)\mathbf{k}_2 \cdot \mathbf{k}_2 = \varepsilon_2 \mu_2, \tag{1}$$

where $\mathbf{k}_2$ is the wave vector in region 2. The solutions must also satisfy a boundary match to the incident wave, requiring

$$\mathbf{n} \times (\mathbf{k}_2 - \mathbf{k}_1) = \mathbf{0}, \tag{2}$$

where $\mathbf{n}$ is the unit normal to the interface. The outgoing, refracted wave must carry energy away from the surface if the incident wave carried energy in,

$$(\mathbf{P}_2 \cdot \mathbf{n})(\mathbf{P}_1 \cdot \mathbf{n}) > 0, \tag{3}$$

where $\mathbf{P} = \frac{1}{2}\mathrm{Re}(\mathbf{E} \times \mathbf{H}^*)$ is the time-averaged Poynting vector. Finally, the wave must not be exponentially growing or decaying, $\mathrm{Im}(\mathbf{k}_2) = 0$, since the media are assumed passive and lossless. If a solution exists that satisfies all the above criteria, the ray is continued with the newfound wave vector and Poynting vector. Furthermore, since we consider only isotropic media, the solution will be unique.

We find that the form of the expressions for the Seidel aberrations of thin spherical lenses found in the optics literature are unchanged by the consideration of negative index media. We reached this conclusion by rederiving these expressions, from first principles, using only the definition of optical path length and Fermat's Principle. We interpret the optical path length, $L_{\mathrm{OP}} = \int_C n(s)ds$, to be the phase change (in units of free-space wavelength) that a wave would undergo along the path C, if C is oriented parallel to the Poynting vector. The optical path may have contributions that are negative where the Poynting vector and the wave vector are

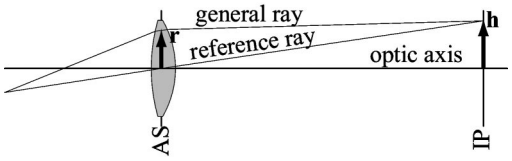

FIG. 1. Construction used for aberration calculation. The aperture stop, labeled AS, is at the plane of the thin lens (although the lens shown is thick). The Gaussian image plane is labeled IP. The aperture stop coordinate vector, **r**, and the image plane coordinate vector, **h**, are not necessarily parallel as shown.

antiparallel, i.e., where the index is negative. These aberration formulas are further corroborated by agreement with the results of our ray tracing.

The wave aberration, ΔL_{OP}, is the difference in optical path length of a general ray and a reference ray, where the reference ray passes through the optic axis in the aperture stop and the general ray is parametrized by its coordinate in the aperture stop, **r**, and its coordinate in the image plane, **h** (Fig. 1). To be in the Gaussian optic limit, where spherical interfaces yield perfect imaging, r and h must be near zero. A series expansion of the wave aberration in these parameters,

$$\Delta L_{\mathrm{OP}} = \sum_{l,m,n=0}^{\infty} C_{lmn}(\mathbf{r}\cdot\mathbf{r})^l(\mathbf{r}\cdot\mathbf{h})^m(\mathbf{h}\cdot\mathbf{h})^n, \tag{4}$$

yields corrections to Gaussian optics of any desired order. The lowest-order corrections for a thin spherical lens with aperture stop in the plane of the lens are given by

$$C_{200} = -\{1/[32f'^3n(n-1)^2]\}[n^3 + (n-1)^2(3n+2)p^2 + 4(n+1)pq + (n+2)q^2], \tag{5a}$$

$$C_{110} = -\frac{1-p}{8f'^3n(n-1)}[(2n+1)(n-1)p + (n+1)q], \tag{5b}$$

$$C_{020} = -[(1-p)^2/8f'^3], \tag{5c}$$

$$C_{101} = -[(1-p)^2/16f'^3n](n+1), \tag{5d}$$

$$C_{011} = 0. \tag{5e}$$

These coefficients are the Seidel aberrations: spherical, coma, astigmatism, field curvature, and distortion, respectively. Also appearing in these expressions are p, the position factor, and q, the shape factor, where we follow the definitions of Mahajan [6]. The position factor is given by

$$p \equiv 1 - (2f'/S'), \tag{6}$$

where f' is the focal length referred to the image side and S' is the image position. Through the thin spherical lens imaging equation,

$$(1/S') - (1/S) = (1/f') = (n-1)[(1/R_1) - (1/R_2)], \tag{7}$$

where S is the object position and R_1 and R_2 are the lens radii of curvature, the position factor is directly related to the magnification,

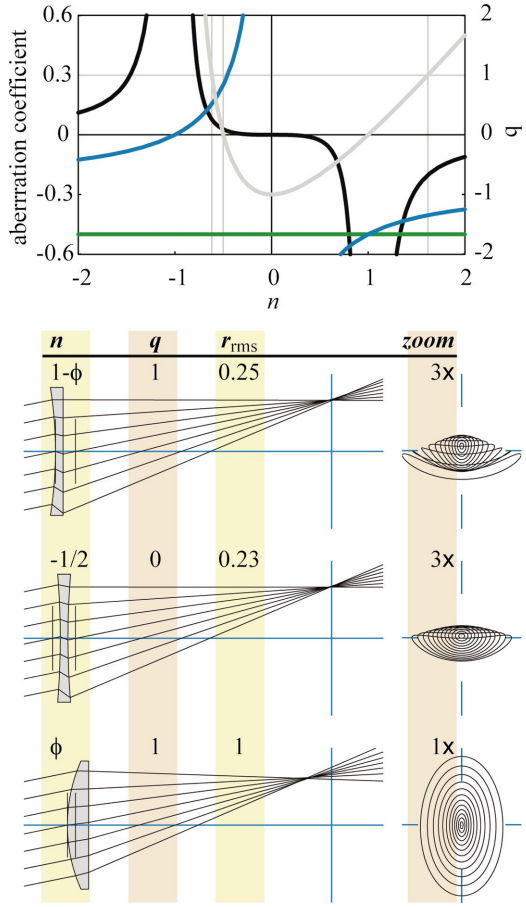

FIG. 2. (Color) The top plot shows spherical aberration (black), astigmatism (green), field curvature (blue), and shape factor (light gray) as a function of index for a lens focusing an object at infinity and bent for zero coma. The thin gray vertical lines indicate properties for lenses shown in ray tracing diagrams (bottom), meridional profile (left), and image spot (right). The incident angle is 0.2 radians and lenses are $f/2$. Index, shape factor, relative rms spot size, and spot diagram zoom are shown tabularly. In the meridional profile, the lens principle planes are shown as thin black vertical lines, and the optic axis and Gaussian image plane are shown as blue lines. In the spot diagram, the Gaussian focus is at the center of the blue cross hairs.

$$M = (S'/S) = [(p+1)/(p-1)]. \tag{8}$$

The shape factor is given by

$$q \equiv (R_2 + R_1)/(R_2 - R_1). \tag{9}$$

A lens with a shape factor of 0 is symmetric, and ±1 is a plano-curved lens. Using the shape and position factor, all thin spherical lens configurations are described.

We will first examine the very important case of a source object at infinite distance. This is a position factor of −1. We are left with two parameters that can be used to reduce aberrations, n and q. We will set the value of q to eliminate one of the aberrations and compare the remaining aberrations as a function of index. We will restrict our attention to moderate values of index. At large absolute values of index, the aberrations approach the same value independent of sign, but dielectric lenses with a high index have significant reflection

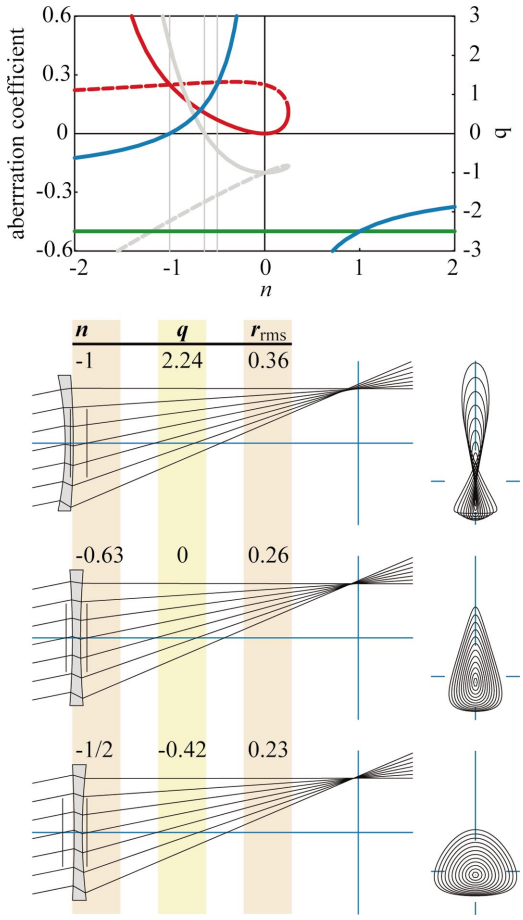

FIG. 3. (Color) All as in Fig. 2, except the following: the lens is bent for zero spherical aberration. The coma is shown in red. The solid and dashed lines indicate different solutions. Spot size, r_{rms}, is relative to the bottom lens spot in Fig. 2. All spot diagrams are at the same scale.

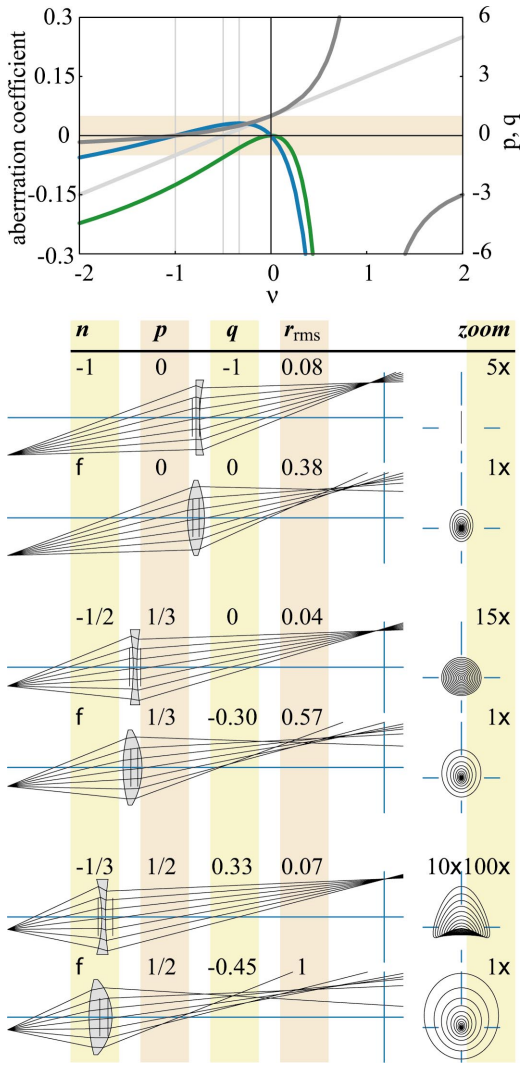

FIG. 4. (Color) All as in Fig. 2, except the following: lens configuration with object and image at finite positions and bent for zero spherical aberration and coma. The position factor is shown in dark gray. Real image object pairs only occur when the position factor is in the shaded region, $|p|<1$. The lens pairs are $f/1.23$, $f/1.08$, $f/0.90$, and have magnifications -1, -2, -3. In the second to last spot diagram, the horizontal $(10\times)$ and vertical $(100\times)$ zooms are not equal.

coefficients due to the impedance mismatch to free space.

The usual ordering of the aberrations is from highest to lowest in the order of r, the aperture coordinate. This is the ordering of greatest to least image degradation, at least if one is forming images with a significant lens aperture, but with a small to moderate image size, which is a common occurrence in applications. Thus, spherical aberration is an obvious target for elimination. However, there are no roots of C_{200} for values of index greater than one, which is why this aberration is referred to as spherical aberration, since it appears to be inherent to spherical lenses. The usual practice is to eliminate coma (the next in line), and it so happens that the resulting lens has a value for the spherical aberration that is very near the minimum obtainable. Adjusting the shape factor, q, is often called lens bending. If we bend the lens for zero coma, that is, find the roots of C_{110} with respect to q, we obtain

$$q_c = [(2n+1)(n-1)]/(n+1). \tag{10}$$

We plug this value for q and $p=-1$ into (5) and plot the remaining three nonzero aberration coefficients as well as q_c in Fig. 2. We note that there are two values of index where $q=1$, which represent a plano-concave/convex lens. Setting (10) equal to one, we obtain

$$n^2 - n - 1 = 0, \tag{11}$$

the roots of which are the ubiquitous golden ratios, $n=\phi \simeq 1.62$ and $n=1-\phi \simeq -0.62$ [8]. We also note that there is a window of index values near $n=-0.7$ where both the spherical aberration and field curvature are small. There is no equivalent window in positive index.

Several ray tracing diagrams with both meridional rays and ray spot diagrams are shown for specific values of index in Fig. 2. The reference lens has an index ϕ, which is close to the typical values used in visible optical lenses and near enough to $n=1$ for reasonably low reflection. The lenses of negative index shown are, in fact, closer to $n=-1$, which is the other index that permits perfect transmission, so this is a

fair comparison. The negative index lenses both show significantly tighter foci than the positive index lens.

If we attempt to bend a lens with $p=-1$ to obtain zero spherical aberration, we obtain the two solutions

$$q_s = [2(n^2-1) \pm n\sqrt{1-4n}]/(n+2). \tag{12}$$

These expressions have real values only for $n \leqslant 1/4$, so an implementation of such a lens (embedded in free space) is not possible with normal materials. It is a surprising and significant result that negative index permits an entire family of spherical aberration-free spherical lenses that can focus a distant object to a real focus (Fig. 3). The solution with the negative sign in the expression for q_s (solid curves) has less coma for moderate negative values of index, so ray tracing diagrams are shown for that solution. We note that at $n=-1$, the field curvature is also zero, thus this lens has only two of the five Seidel aberrations, coma and astigmatism. For a positive index reference we use the zero coma, $n=\phi$ lens from above. Here again, negative index lenses achieve a tighter focus than a comparable positive index lens.

Now we examine the case of $|p|<1$, that is, a real object and real image both at finite position. Since p and q are both free parameters, we can conceivably eliminate two aberrations. If we eliminate spherical aberration and coma, the resulting lens is called *aplanatic*. It is a well-known, though incorrect, result that a spherical lens can only have *virtual* aplanatic focal pairs. The correct statement is that only negative index spherical lenses can have *real* aplanatic focal pairs.

If we set C_{200} and C_{110} to zero and solve for p and q, we obtain four solutions, the two nontrivial ones are given by

$$p_{sc} = \mp [(n+1)/(n-1)], \tag{13a}$$

$$q_{sc} = \pm (2n+1). \tag{13b}$$

We will focus on the solution with a minus sign for p and the plus sign for q. This solution has smaller aberrations for lens configurations that magnify an image. The other solution is better for image reduction. Inserting expressions (13) into (5) we have plotted the two remaining nonzero coefficients, as well as the values of p_{sc} and q_{sc} (Fig. 4). Ray diagrams are shown for lenses with magnifications of -1, -2, and -3. Also shown is a reference positive index lens for each. The reference lenses (which cannot be aplanatic) are of moderate index, ϕ, with the same magnification and $f/\#$ as the lenses to which they are compared. They are bent for zero coma but also have spherical aberration near the minimum possible for the configuration. Again, the negative index lenses produce superior foci.

The lens of index -1 and magnification -1 is particularly interesting. At this index value, the field curvature is also zero. This remarkable lens configuration has only one of the five Seidel aberrations, astigmatism. This is confirmed by ray tracing, which shows a one-dimensional "spot" at the image plane. This is perfect focusing in the sagittal plane. Perfect focusing also occurs in the meridional plane, in front of sagittal focus.

One may ask why this asymmetric lens, $q=-1$, performs so well in a symmetric configuration, $p=0$. This lens can be equivalently viewed as a biconcave doublet with one component having index -1 and the other having index 1, i.e., free space. Driven by this observation, we found that all biconcave doublets with arbitrary indices of $\pm n$ have identical focusing properties. The only observable difference is in the internal rays, which are always symmetric about the planer interface, but make more extreme angles at higher index magnitude.

Fabrication of any of these negative index lenses is quite feasible using periodically structured artificial materials. Current artificial material designs can operate at frequencies from megahertz through terahertz [9], where there are numerous communication and imaging applications. For example, lens antennas could benefit both by a reduction in aberrations, which translates directly into increased gain, and by a reduction of mass, afforded by low-density artificial materials. (Antenna applications of artificial materials have both historical and recent [10] interest.) Furthermore, these lenses are even easier to implement than a perfect lens, since they lack its severe structure period per wavelength requirements and are more tolerant to losses [11]. Negative index lenses at visible light frequencies may also be possible, by using photonic crystals, which have shown potential for negative refraction [12,13].

Using the current optical system design paradigm, aberrations are minimized by combining elements with coefficients of opposite sign [14]. However, more elements mean greater complexity and cost. Taking advantage of an expanded parameter space that includes negative index can reduce the number of required elements—possibly even to one.

This research was supported by DARPA (Contract No. MDA972-01-2-0016) and a Multiple University Research Initiative (MURI), sponsored by ONR (Contract No. N00014-01-1–0803).

[1] V. G. Veselago, Sov. Phys. Usp. **10**, 509 (1968).
[2] D. R. Smith *et al.*, Phys. Rev. Lett. **84**, 4184 (2000).
[3] J. B. Pendry, Phys. Rev. Lett. **85**, 3966 (2000).
[4] A. Lakhtakia, Int. J. Infrared Millim. Waves **23**, 339 (2002).
[5] C. G. Parazzoli *et al.*, Appl. Phys. Lett. **84**, 3232 (2004).
[6] V. N. Mahajan, *Optical Imaging and Aberrations*, 1st ed. (SPIE, Bellingham, WA, 1998), Vol. I.
[7] B. Kress and P. Meyrueis, *Digital Diffractive Optics: An Introduction to Planar Diffractive Optics and Related Technology*, 1st ed. (Wiley, Hoboken, NJ, 2000).
[8] M. Livio, *The Golden Ratio: The Story of PHI, the World's Most Astonishing Number*, 1st ed. (Broadway, 2003).
[9] T. J. Yen *et al.*, Science **303**, 1494 (2004).
[10] S. Enoch *et al.*, Phys. Rev. Lett. **89**, 213902 (2002).
[11] D. R. Smith *et al.*, Appl. Phys. Lett. **82**, 1506 (2003).
[12] E. Cubukcu *et al.*, Nature (London) **423**, 604 (2004).
[13] P. V. Parimi *et al.*, Nature (London) **426**, 404 (2004).
[14] E. Hecht, *Optics*, 3rd ed. (Addison-Wesley, Reading, MA, 1998).